Evolution Strategies for Computational and Experimental Fluid Dynamic Applications

Ivo F. Sbalzarini **Sibylle D. Müller** **Petros D. Koumoutsakos** **G.-H. Cottet**
Institute of Computational Sciences
Swiss Federal Institute of Technology
CH - 8092 Zürich, Switzerland
{ivos,muellers,petros}@inf.ethz.ch

LMC-IMAG
Université Joseph Fourier
Grenoble, France

Abstract

Evolution strategies are developed and implemented to optimization problems in Fluid Dynamics applications. We consider two- and multimembered evolution strategies as applied to fluid dynamic problems over a large range of scales, studied computationally (trailing wake aircraft vortices and micromixers) as well as experimentally (jet mixing control). The implementation of the algorithms in an experimental or computational environment is discussed. The results demonstrate that evolution strategies are effective optimization techniques for these complex fluid dynamic applications.

1 Introduction

We apply evolution strategies (ES) to three selected optimization problems in fluid dynamics. The first and second application employ numerical simulations of the problem studied while the third application is performed in an experimental setup. First, we consider the problem of trailing aircraft wake destruction by modifying perturbation parameters modeling flap movements. The vortex wake is simulated using vortex methods (see section 2). Second, we optimize a microfluidic device used for medical applications. Our goal is to enhance the mixing rate in a micromixer by combining an optimization strategy with a simulation of the flow in the mixer (see section 3). Third, we present the optimization of a jet in an experimental setup. In this example, it is intended to enhance the mixing of the jet by finding optimal actuation parameters (see section 4) in an automated fashion.

We use both a (1+1)-ES with the 1/5-success rule for step size adaptation [Rechenberg (1994)] and a derandomized $(\mu/\mu_I, \lambda)$-CMA-ES using covariance matrix adaptation and intermediate recombination [Hansen & Ostermeier (1997)]. A hybrid technique is also been investigated.

2 Computation: Optimization of trailing vortex destruction

2.1 Problem description

Trailing vortices are naturally shed by airplanes. They result in a strong down-wash that extends for several miles behind the plane and poses a hazard to following aircraft, in particular at take-off and landing. Several previous studies propose to alleviate the hazard by introducing flap induced perturbations to trigger instabilities, and ultimately, break up the vortices [Bilanin & Widnall (1973)], [Crow & Bate (1997)].

Most of these studies have focused on exciting the Crow instability that operates on a single pair of counter-rotating vortices and has a wavelength much larger than the vortex core size. Unfortunately, however, for realistic perturbation amplitudes (those which would not cause large unsteady forces on the plane) excitation of the Crow instability would lead to vortex destruction at large distances behind the plane.

Recent works [Rennich & Lele (1998)],[Crouch (1997)] have considered instabilities unique to several pairs of vortices which model aircraft wakes in landing configuration [Spalart (1998)], see Fig. 1. Some of these vortices quickly merge but others persist for long times. At a distance of several spans behind a typical airplane, three persistent vortex pairs can generally be observed, originating at the tips of the wings, the outboard flaps, and the fuselage (respectively numbered 50, 52, and 55 in Fig. 1). [Crouch (1997)] has studied the linear stability of two pairs of corrotating vortices (tip and outboard flap, 50 and 52 in Fig. 1). He identi-

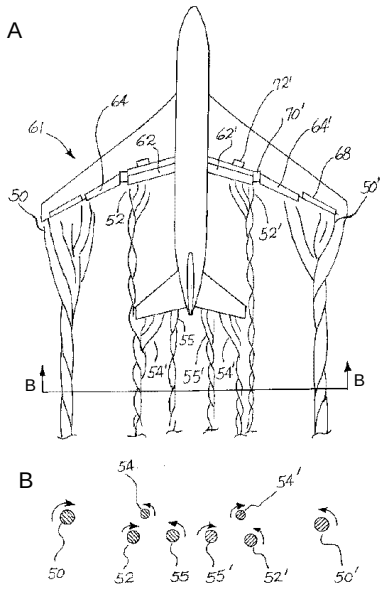

Figure 1: Sketch of vortex system shed by an airplane (Courtesy of J. Crouch, 2000). B is a cross section of A as shown.

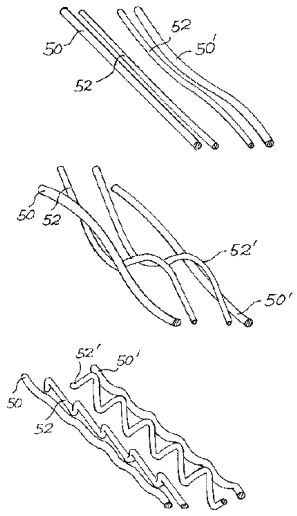

Figure 2: Three types of instabilities according to [Crouch (1997)]. From top to bottom: long wave, transient growth, and short wave instabilities.

fied several instability modes depending on the angle, wavelength, and amplitudes of the perturbations that are imparted to each pair by the flap. The modes are summarized in Fig. 2. In general, a long wave instability (top sketch in Fig. 2), similar to the Crow instability, takes place when the two pairs are excited in a symmetric fashion. An instability with a wavelength shorter than that for the Crow instability (but still much longer than the core size) can also result (bottom sketch). The most efficient instability (middle sketch) arises when the eigenmodes are non-orthogonal, leading to transient growth rates exceeding the maximum eigenvalue. This instability mechanism produces long waves which, when the outboard vortices are initially unperturbed, grow at a rate several times larger than the Crow instability for a single vortex pair.

Based on the analysis of [Crouch (1997)], [Crouch & Spalart (2000)] propose a strategy for breaking up the vortices that relies on appropriate oscillations of the control surfaces. Their experiments and numerical simulations indicate that this strategy could induce the growth of a destructive instability.

One of the findings reported in [Crouch (1997)] and [Rennich & Lele (1998)] is the extreme sensitivity of the overall dynamics with respect to the initial state of the vortex pairs. In [Crouch (1997)], the most effective transient growth was achieved when the outboard pair was not initially perturbed, while in [Rennich & Lele (1998)] early reconnection was obtained for a particular value of the inboard vortices separation.

This motivated our attempt to perform a more systematic parameter search and identify the wake system which would produce the largest instability growth. The tools used in this work are ES's and viscous vortex methods [Cottet & Koumoutsakos (2000)]. ES's are used here for the optimization of the full nonlinear problem as opposed to the linearized situations studied by the previous works.

2.2 Results

Our work focused on the case of two pairs of corotating vortices studied by [Crouch (1997)]. The seven optimization parameters were the initial perturbation amplitude of the tip (ϵ_1) and outboard (ϵ_2) vortices, the angles of the perturbation planes α_1 and α_2, the wavelength of the perturbations, λ, the separation between the two vortices, δ, the circulation ratio between the outboard and tip vortices, Γ. Quantities were non-dimensionalized by the distance b_0 between the tip vortices and the total circulation. To work with parameters in the same order of magnitude as [Crouch (1997)], the total perturbation amplitude was constrained to be below 10% of b_0: $\sqrt{\epsilon_1^2 + \epsilon_2^2} \leq 0.1$. Parameter limits are $0.25 \leq \delta \leq 0.4$; $0.5 \leq \lambda \leq$

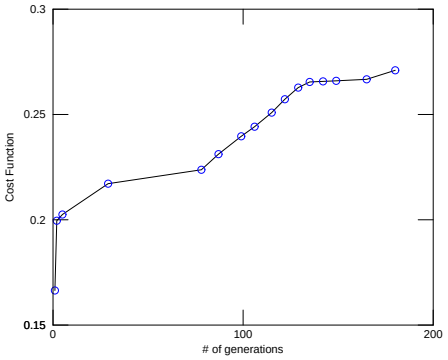

Figure 3: Convergence history for the evolution strategy.

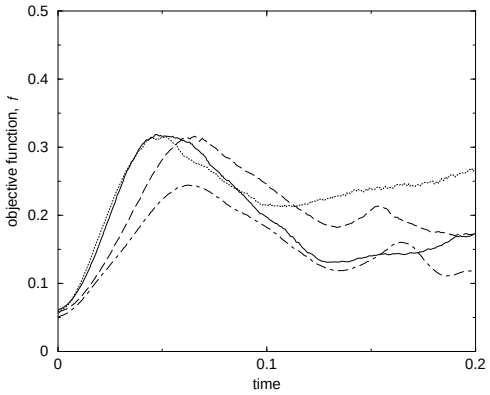

Figure 4: Evolution of the objective function. solid: optimal parameters for 2 pairs by ES; dashed: parameters of [Crouch (1997)]; dotted: optimal parameters for 4 pairs by ES; chain-dot: 2 pairs of equal initial perturbation.

α_1	α_2	ϵ_1	ϵ_2	δ	Γ	λ
0.47	0.73	0.098	0.008	0.26	0.31	0.72
$\pi/4$	$\pi/4$	0.1	0.	0.3	0.4	0.7

Table 1: Comparison of the parameters found by the evolution strategy (top row) and those studied in [Crouch (1997)] (bottom row).

10; $0. \leq \Gamma \leq 0.5$. Note that the boundaries of λ allow for a wide range of wavelengths, varying from short wavelengths of the order of a few core sizes to long wavelengths of the type found in the Crow instability.

Our goal was to maximize the instability on the tip vortex. To measure its deformation, we computed the average angle, inside the core of the tip vortex, of the vorticity vector relative to the axis of the unperturbed vortex.

Figure 3 shows the convergence history of the algorithm, a hybrid technique using the (1+1)-ES in the early generations, followed by the CMA-ES.

The parameter values finally obtained by the ES are listed in Table 1 (top row) together with the parameters reported in [Crouch (1997)] as leading to efficient transient growth (bottom row). Some striking similarities can be noticed between these two sets of parameters. In particular, the ES has selected perturbations that are mostly located on the tip vortex, confirming the observation in [Crouch (1997)] of efficient transient growth when the outboard flap vortex was unperturbed. The wavelengths of the perturbations are also very close to the ones given in [Crouch (1997)].

Finally, Fig. 4 shows the evolution of the objective function for various parameter vectors: the two sets of parameters shown in Table 1, parameters similar to the ones found by the ES but with perturbations of same magnitude for the two pairs and a third set of parameters obtained by optimizing on 4 pairs instead of 2 pairs. These simulations confirm that, in the early stages of the dynamics, the ES has picked up the most efficient parameters for two pairs. However, an inspection of the vorticity angle at later times show that the differences between the configurations involving pairs of co-rotating pairs tend to disappear. A similar observation was made in [Rennich (1997)] by considering a different measure of the perturbation (namely the maximum displacement). Clearly, the cost function behavior is unsteady and non-monotonic. Therefore, care must be exercised when interpreting the results of the optimum parameters. One can also notice that adding more degrees of freedom to the optimization can pay off and lead to increased efficiency, as found by the ES.

3 Micromixer Optimization

The CMA-ES with strategy parameters as described in [Hansen & Ostermeier (1997)] is applied to optimize a micromixer. Since we are dealing with a highly dynamical system that introduces noise to the objective function, we take advantage of the recombination feature in the proposed method.

The proposed mixer is actively controlled to enhance mixing in a straight channel. Flow in the main channel is manipulated by controlling time-dependent flow from six secondary channels. From these secondary channels, time-dependent cross-flow momentum is im-

parted on the main channel flow which alters the trajectories of flow-tracing particles. The flow configuration is illustrated in Figure 5.

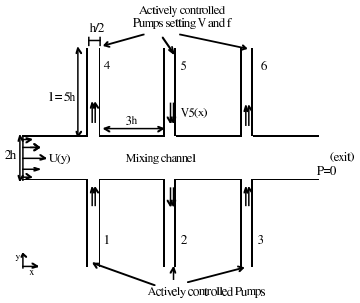

Figure 5: Schematic of the flow configuration

The inlet velocity $U(y)$ of the main channel is parabolic, and the inlet velocity of each secondary channel set i

$$V_i = \hat{V}_i \sin(2\pi f_i t + \phi_i), i = 1, 2, 3 \qquad (1)$$

is sinusoidal in time where f_i is the oscillation frequency, ϕ_i the phase shift relative to the first set of secondary channels, and $\hat{V}_i$ the velocity amplitude.

In order to study the performance of the mixer, we compute the mixing rate of the flow by numerical simulations of the governing Navier-Stokes equations at a Reynolds number $Re = 5$.

The aim of the optimization is to obtain the parameter vector which leads to the most pronounced mixing rate in the micromixer. Actuation parameters are the frequency, the amplitude, and the phase shift for each pair of the secondary channels, yielding a total number of 9 actuation parameters. Within this work, we set amplitudes and phases to constant values, namely $\hat{V}_1 = \hat{V}_2 = \hat{V}_3 = 2U_m = 2$, and $\phi_1 = \phi_3 = 0$, $\phi_2 = \pi$ as recommended in [Volpert, Mezic, Meinhart & Dahleh (2000)]. As optimization parameters remain the three frequencies f_1, f_2, f_3 which vary within the limits $[0, 1]$, summarized in the parameter vector $\mathbf{x} = (f_1, f_2, f_3)$.

The objective function to be minimized is the mixing rate m, based on the the scalar concentration and the number of vertices in the outlet for which the concentration is measured.

For the optimization, we average the mixing rate in a time regime in which the flow reaches steady state for the tested frequencies. The CPU time for one simulation takes about 3 CPU hours on a Sun Sparc Ultra-2 processor. Using MPI, the optimization is run in parallel on 5 processors of a Sun workstation cluster.

The results of the optimization of the three frequencies are documented in Table 2.

Table 2: Initial and optimized frequencies

Number of actuated frequencies		3
Initial frequencies	f_1	0.25
	f_2	0.3333
	f_3	0.5
Initial mixing rate	m	0.0345
Best frequencies	f_1	0.1388
	f_2	0.3165
	f_3	0.4956
Best mixing rate	m	0.0213
Number of function evaluations		460

To obtain the required accuracy of the parameters, the function had to be evaluated 460 times. Due to the huge computational cost of the optimization, we could not afford to run another optimization with a different direct search technique and compare it with the ES. However, we compare the optimization result with dynamical system theory. The optimum frequency for a mixer with only one side channel can be determined analytically by considering the movement of a fluid particle in the main channel which yields a value of $f = 1/2$ (non-dimensional units). From studying the ratios of the frequencies, one can learn that there is a difference if frequency ratios are 1, rational, or irrational. The computation of the mixing rate for the parameter vector $\mathbf{x} = (1/2, 1/2, 1/2)$ with identical frequencies yields $m = 0.1596$ while our initial "rational" frequency set $\mathbf{x} = (1/2, 1/3, 1/4)$ gives us $m = 0.0345$. "Irrational" frequencies as proposed in [Volpert, Mezic, Meinhart & Dahleh (2000)] $\mathbf{x} = (1/(2\sqrt{5}), 1/(2\sqrt{2}), 1/2)$ yield $m = 0.0285$ which is the best mixing found theoretically. As one can see, the evolutionary optimization yields a much better mixing rate of $m = 0.0213$ with the frequencies reported in Table 2. This result means a considerable improvement compared with numbers from a well-established theory.

Figures 6 and 7 show a snapshot of the flow in the micromixer for the identical and optimal frequencies, respectively.

4 Experiments: Jet Control

We are reminded here that ES's were first developed and implemented for parameter optimization in experimental fluid dynamics studies by Rechenberg and Schwefel [Rechenberg (1994)]. In this paper, we revisit the application of ES's to experiments while tak-

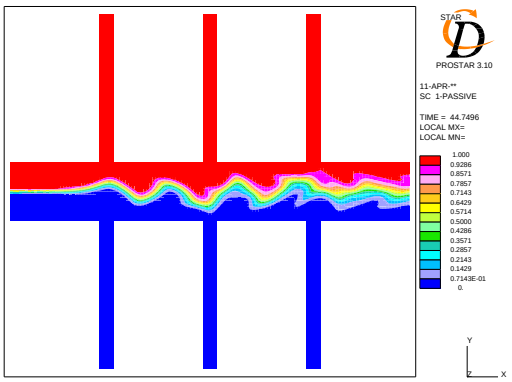

Figure 6: Flow actuated by $\mathbf{x} = (1/2, 1/2, 1/2)$

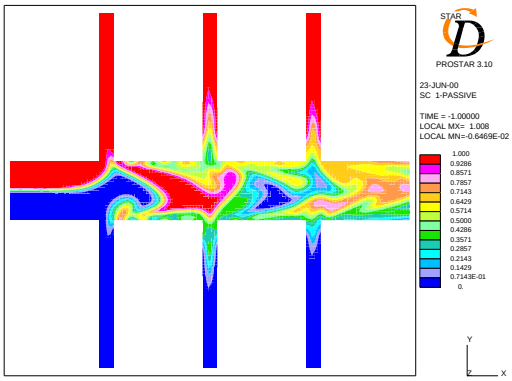

Figure 7: Flow actuated by optimal frequencies

ing advantage of modern experimental tools, resulting in fully automated experiments for the problem of jet mixing at high Reynolds numbers.

An automatic experiment driven by evolution consists at least of the following functional blocks: the experimental hardware setup itself, hardware computer interfaces such as D/A and A/D converters, a general purpose digital computer, a data acquisition and control software, an ES code and a communication interface between the ES code and the acquisition/control software.

Data acquisition and control software are the only connection of the ES code to the real, physical world. For this work, National Instrument's LabView 5.1 has been used. It was set up to control the whole experiment in its sequential course and collect all the measurement data needed.

For the optimization, a restartable (1+1)-ES has been implemented with a communication subroutine connected to LabView. The evolution code and LabView run on the same computer in multitasking mode that allows them to be executed concurrently. Both LabView and the ES code write and read shared files to exchange information or monitor flag files for the sake of synchronization.

Applying evolution to experiments means coping with additional effects that are usually not present in computation. They can roughly be divided into effects caused by measurement uncertainties (or errors), digital signal quantification and uncontrollable environmental influences.

4.1 Problem description

The method of evolutionary experiments has been applied to the control of a high Reynolds number round air jet. This problem has been chosen because it is a quite well known issue for which many references from conventional experiments (e.g. [Parekh, Leonard & Reynolds (1988)], [Parekh, Kibens, Glezer, Wiltse & Smith (1996)] and [Juvet & Reynolds (1993)]) as well as from computational studies (e.g. [Freund & Moin (1998)]) are available.

The experimental setup consists of a vertical jet of warm (about 35°C) air exiting from a straight nozzle (inner diameter $D = 20\,\mathrm{mm}$). The surrounding air was air-conditioned to about 20°C. Temperature profiles were measured on a straight path from the center of the jet outwards using a type K thermocouple connected to a Fluke thermocouple adaptor. The thermocouple was moved across the jet $l = 122.2\,\mathrm{mm}$ ($l/D = 6.11$) above the nozzle exit. The jet was acoustically excited using 5 loudspeakers. 4 of them were used to create a helical excitation of certain frequency, amplitude, and phase and one was used to create an axial excitation. Detailed descriptions of the setup and the hardware can be found in [Parekh, Leonard & Reynolds (1988)], [Parekh, Kibens, Glezer, Wiltse & Smith (1996)], and [Juvet & Reynolds (1993)]. The inputs of the amplifiers driving the speakers were connected to the outputs of D/A converters which in turn were connected to the computer. The temperature sensor was mounted on an arm and moved across the jet by a step motor, controlled by the computer. The speed of this transverse motion is basically what controls the speed of each cost function evaluation. Temperature readings at each point were digitized and fed to the computer. Temperatures were measured at certain

distances from the center of the jet, collecting 3000 samples per point at a sampling rate of 500 Hz.

The jet was acoustically excited using two different modes: helical and axial. The helical excitation was done by four speakers, regularly arranged around the centerline of the jet (i.e. the angle between adjacent speakers was 90°). Their sound was fed into the jet right before the exit nozzle using wave guides. The excitation signal was sinusoidal, the phase corresponded to the geometrical setup, i.e. one speaker was fed a sine wave, the one to its right a cosine wave, the one opposite of it a negative sine wave and the one to its left a negative cosine wave. Therefore, the phase between adjacent speakers was 90° in normal operation mode. However, this phase could be shifted by adding some value. Opposite speakers were always 180° out of phase, regardless of the phase shift between adjacent ones. The two pairs of opposite speakers (i.e. the ones fed with a sine wave and the ones fed with a cosine wave) were connected to two different channels of the same power amplifier. Phase reversal for opposite speakers was done by simply changing the polarity of the wires. The amplifier was adjusted to a gain of 60, which corresponds to a maximum output amplitude of $16\,\mathrm{V_{RMS}}$.

The axial excitation was done by a single loudspeaker sitting in the bottom of the jet column. It was connected to the output of a second power amplifier and fed with a simple sine wave of specific frequency. The amplifier was adjusted to a gain of 30 which corresponds to a maximum output amplitude of $16\,\mathrm{V_{RMS}}$, too. The frequency range of the 5 speakers was 300 Hz to 3000 Hz. The amplitudes and frequencies for both modes as well as the phase shift of the helical excitation are controlled by the computer.

The optimization parameters are: the frequency of helical excitation (f_h) in Hertz, the frequency of axial excitation (f_a) in Hertz, the amplitude of helical excitation (A_h) in Volts, the amplitude of axial excitation (A_a) in Volts, and the phase shift of helical excitation (φ) in radians. The parameters are subject to the following boundaries of the search space: both frequencies have to be between 300 Hz and 3000 Hz (band limits of the speakers), both amplitudes have to be between $0\,\mathrm{V_{RMS}}$ and $16\,\mathrm{V_{RMS}}$ (amplifier power limitation).

The goal is to maximize the spreading angle of the jet which is strongly correlated to mixing. Therefore, the fitness function was chosen to be proportional to the discrete variance of the normalized temperature profile.

To see whether a certain experiment can be treated by evolution using a given fitness function, a variance analysis should be performed. One simply measures the fitness values at certain, fixed points in parameter space several times to get an estimate of mean and variance at these points. From our variance analysis, we concluded that the variation due to measurement uncertainties seems to be small enough to allow evolution with an accuracy of at least one unit in fitness value. This means that if the difference in fitness of two parameter vectors is more than one, it can be considered a significant difference and one parameter set is clearly better then the other.

4.2 Results

Two runs under different conditions were performed for the jet. The amplitudes have been fixed to their maximum allowable values for all runs. In the first run presented here, both frequencies have been varied independently, the phase shift was fixed to 0, and the evolution started from a random point. In the second run, the frequency ratio has been optimized starting from the "strong blooming" condition found by [Juvet & Reynolds (1993)].

4.2.1 Run 1: Two frequencies at Re = 102000

Both frequencies were optimized while the amplitudes were fixed at their maximum of $A_a = 16\,\mathrm{V_{RMS}}$ and $A_h = 16\,\mathrm{V_{RMS}}$. The phase shift was fixed at 0 which means that adjacent speakers were 90° out of phase. The initial step sizes for the ES were 50 Hz for both frequencies and step size adaptation was done every 20 generations. The temperature was measured at 8 points at distances of $0, 5, 10, 15, 20, 30, 40$ and 50 mm from the center of the jet (i.e. at $d/D = 0, 0.25, 0.5, 0.75, 1, 1.5, 2, 2.5$). 3000 samples at 500 Hz sampling rate were taken at each point, which corresponds to a sampling time of 6 seconds. Statistical analysis has shown that this sampling time is sufficient to get a stable mean within 1%. The Reynolds number based on the inner diameter of the exit nozzle is $Re_D = 102000$ for this run. The starting values for the parameters were: helical frequency $f_h = 1000\,\mathrm{Hz}$ and axial frequency $f_a = 1800\,\mathrm{Hz}$ which corresponds to Strouhal numbers (based on the inner diameter of the exit nozzle) of $St_h = 0.26$ and $St_a = 0.46$, respectively. The initial fitness value at this point was 6.8.

The ES was run for 100 generations. Figure 4.2.1 shows the obtained (not the best!) fitness values in each generation of the ES. The best parameter vector has been found at generation 48 as $f_h = 777\,\mathrm{Hz}$

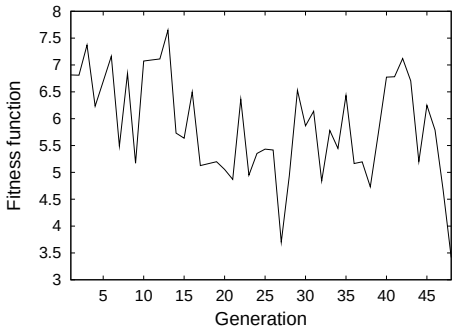

Figure 8: Path of (1+1)-ES

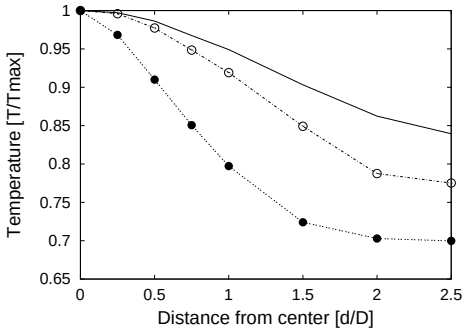

Figure 9: Normalized temperature profiles of natural jet (—●—), initial condition for ES (—○—) and best result of ES (——)

($St_h = 0.20$), $f_a = 1773\,\mathrm{Hz}$ ($St_a = 0.45$) and had a fitness value of 3.4 which is half of the fitness value at the starting point. Figure 4.2.1 shows the temperature profiles (normalized to the peak temperature) for initial and best parameters as well as for the natural jet without any excitation. The profiles got flatter, which means a higher spreading of the jet. The results found by the ES are consistent with prior studies since it has been shown numerically by [Freund & Moin (1998)] that strong flapping of the jet appears for $St_h = 0.2$. The same has been observed in experiments by [Parekh, Kibens, Glezer, Wiltse & Smith (1996)]. Moreover, a large amplification of signals was observed by [Parekh, Kibens, Glezer, Wiltse & Smith (1996)] and [Parekh, Leonard & Reynolds (1988)] for $St_a \approx 0.4$. The same Strouhal numbers have also been found in the first attempt to find optimal actuation parameters for compressible jets with numerical simulations and ES by [Koumoutsakos, Freund & Parekh (1998)]. This suggests that the ES has found reasonable parameters in this case.

4.3 Run 2: Frequency ratio at Re = 95000

In this run, the frequency ratio was optimized while the frequency of the axial excitation has been fixed at 2060 Hz ($St_a = 0.56$). Both amplitudes were fixed at their maximum values of 16 V_{RMS} each and the phase shift was fixed at 0 again. The helical frequency was varied by the (1+1)-ES starting from 896 Hz ($St_h = 0.24$) with an initial step size of 50 Hz. Step size adaptation was performed every 10 generations. The starting values for this run correspond to a frequency ratio of 2.3 which is clearly within the range for blooming ([Lee & Reynolds (1985)]). They are identical to the parameters of the "strong blooming" condition that have been found by [Juvet & Reynolds (1993)] as a condition of very high spreading. They also fixed the axial frequency to 2060 Hz and run at the same Reynolds number. The only differences between their measurements and the present work are that they used a shrouded jet (which should not have any influence on the position of the optimum, however) and hot-wire velocity measurements instead of temperature measurements. The initial fitness value for the strong blooming point was found to be 8.3.

The ES was run for 100 generations. Figure 10 shows the obtained (not the best!) fitness values in each generation of the ES. The best parameter vector has been found at generation 25 as $f_h = 791\,\mathrm{Hz}$ ($St_h = 0.21$), which corresponds to a frequency ratio of 2.6 and a fitness value of 4.5. Compared to the initial fitness value of 8.3, this is again a significant improvement. Figure 11 shows the temperature profiles (normalized to the peak temperature) for initial (strong blooming) and best parameters as well as for the natural jet without any excitation. Even compared to the "strong blooming" condition, the evolution has achieved a significant improvement.

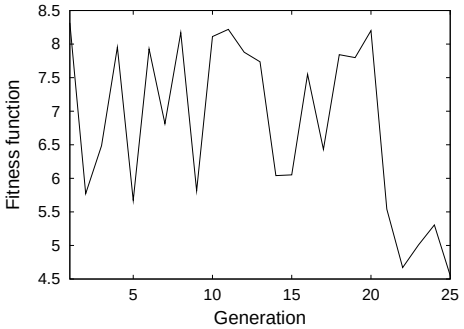

Figure 10: Path of (1+1)-ES

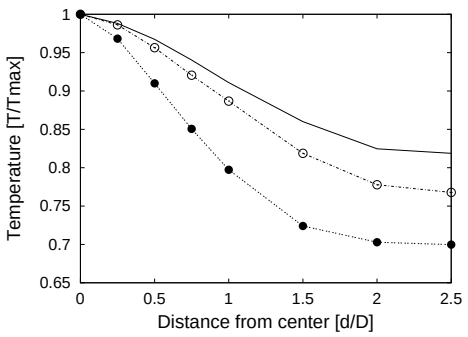

Figure 11: Normalized temperature profiles of natural jet (—●—), strong blooming condition (—○—) and best result of ES (——)

5 Conclusions

Our goal was to optimize three fluid dynamic applications, namely the enhancement of vortex break-up, the mixing in microdevices, and the control of jets. In all applications, we achieved results that outperform existing solutions or theoretical results. We showed that ES's can be a valuable tool to optimize multi-scale fluid dynamic problems in both simulations and experiments.

References

[Bilanin & Widnall (1973)] Bilanin, A. J. & Widnall, S. E., 1973, Aircraft wake dissipation by sinusoidal instability and vortex breakdown. *AIAA Paper 73-107.*

[Cottet & Koumoutsakos (2000)] Cottet, G.-H. & Koumoutsakos, P., 2000, *Vortex methods.* Cambridge University Press.

[Crouch (1997)] Crouch, J. D. , 1997, Instability and transient growth for two trailing-vortex pairs. *J. Fluid Mech.* **350**, 311-330.

[Crouch & Spalart (2000)] Crouch, J. D. & Spalart, P. R., 2000, Active system for early destruction of trailing vortices. *US Patent 6082679* issued July 4, 2000.

[Crow & Bate (1997)] Crow, S. C. & Bate, E. R., 1976, Lifespan of trailing vortices in a turbulent atmosphere. *J. Aircraft.* **13**, 476-482.

[Freund & Moin (1998)] Freund, J. B. & Moin, P., 1998, Mixing enhancement in jet exhaust using fluidic actuators: direct numerical simulations, ASME: FEDSM98-5235.

[Hansen & Ostermeier (1997)] Hansen, N. & Ostermeier, A., 1997, Convergence Properties of Evolution Strategies with the Derandomized Covariance Matrix Adaptation: The $(\mu/\mu_I, \lambda)$-CMA-ES, *Proceedings of the 5th European Conference on Intelligent Techniques and Soft Computing (EUFIT '97)*, 650-654.

[Juvet & Reynolds (1993)] Juvet, P. J. D. & Reynolds, W. C., Sept. 1993, Control of high Reynolds number round jets, *Report No. TF-59, Thermosciences Division, Dept. of Mechanical Engineering, Stanford University*, Supported by the Air Force Office of Scientific Research under contracts AF-F49620-86-K-0020 and AF-91-072-A.

[Koumoutsakos, Freund & Parekh (1998)] Koumoutsakos, P. D., Freund, J. B. & Parekh, D., 1998, Evolution Strategies for Parameter Optimization in Jet Flow Control, *Proceedings of the 1998 Summer Research Program*, Center for Turbulence Research, Stanford University.

[Lee & Reynolds (1985)] Lee, M. & Reynolds, W. C., 1985, Bifurcating and Blooming jets, *Report No. TF-22, Thermosciences Division, Dept. of Mechanical Engineering, Stanford University.*

[Parekh, Kibens, Glezer, Wiltse & Smith (1996)] Parekh, D., Kibens, V., Glezer, A., Wiltse, J. M. & Smith, D. M., 1996, Innovative Jet Flow Control: Mixing Enhancement Experiments, *34th Aerospace Science Meeting*, Reno, AIAA paper 96-0308.

[Parekh, Leonard & Reynolds (1988)] Parekh, D., Leonard, A. & Reynolds, W. C., 1988, Bifurcating jets at high Reynolds numbers, *Report No. TF-35, Thermosciences Division, Dept. of Mechanical Engineering, Stanford University.*

[Rechenberg (1994)] Rechenberg, I., 1994, Evolutionsstrategie 94, Frommann-Holzboog, Stuttgart.

[Rennich (1997)] Rennich, S. C., 1997, Accelerated destruction of aircraft wake vortices. *Ph.D. thesis*, Stanford.

[Rennich & Lele (1998)] Rennich, S. C. & Lele S. K., 1998, A method for accelerating the destruction of aircraft wake vortices. *AIAA Paper* 98-0667.

[Spalart (1998)] Spalart, P. R., 1998, Airplane trailing vortices. *Ann. Rev. Fluid Mech.* **30**, 107-138.

[Volpert, Mezic, Meinhart & Dahleh (2000)] Volpert, M., Mezic, I., Meinhart, C.D. & Dahleh, M., 2000, Modeling and Analysis of Mixing in an Actively Controlled Micromixer, *University of Santa Barbara, Internal Report.*